International Journal of Civil Engineering and
Geo-Environmental

Journal homepage:http://ijceg.ump.edu.my
ISSN:21802742

FOUR-DIMENSIONAL OF TSUNAMI DISASTERS EFFECTS UTILIZING HOLOGRAM INTERFEROMETRY OF SATELLITE DATA

M. Marghany[1*]

[1]Geospatial Information Science Research Center, Faculty of Engineering, Universiti Putra Malaysia, Selangor, Malaysia

ARTICLE INFO

Keywords:

QuickBird satellite
Kalutara coastline
4-D phase unwrapping
N-dimensional
Hologram interferometry

ABSTRACT

This work aims at using hologram interferometric with 4-D phase unwrapping to reconstruct fourth-dimensional of box-day Tsunami 2004 impacts on Kalutara coastline. The data are used that involved two QuickBird images with implementation of 4-D phase unwrapping. The results show that the hologram Interferometric an excellent tool for reconstructing tsunami chaotic effects on land uses from QuickBird satellite data. The study shows coastline of Kalutara is flooded by tsunami run-up of 6 m which totally damaged road network and urban structures. Hologram interferometry able to reconstruct 4-D of coastal water turbulent flows along Kalutara coastline. In conclusion, 4-D view of tsunami coastal damages can be reconstruct using the optical hologram Interferometric from QuickBird satellite data.

1. Introduction

Yet advanced remote sensing technology does not implement n-dimensional and simply restricted to three-dimensional. Conversely, n-dimensional is curious topic between mathematicians and physicians. Up until currently, standard remote sensing technology disables to implement n-dimensional and is simply forced to simulate three-dimensional of any ground object. Though, n-dimensional is recently and riveted theme for mathematicians and physicians. String theory, M-theory, and Supergravity square measure most accepted n-dimensional theories. String theory, consequently, planned that the universe is formed in multiple dimensions: (i) height; (ii) width; associate degreed (iii) length compose three-dimensional space; and (iv) time contributes a completeness of 4 discernible dimensions. String theories, notwithstanding, continuing the probability of 10 dimensions – the remaining six of that human capability cannot depiction exactly (Alday et al., 2010; Marghany, 2015).

Though, the pure mathematics of four-dimensional (4-D) space is an abounding further convoluted than that of three-dimensional space, attributable to the extraordinarily degree of freedom. Consequently, 4-D involves 4-polytopes that square measure developed of polyhedral (Figure 1). Additionally, 4-D conjointly contains 6 convex regular 4-polytopes that are the analogues of the Platonic solids. Therefore, as 3-D beings it cannot transfer freely in time, however in 4-D it can be realizable. In this context, 4-D can distinguish three-dimensional and it cannot be conveyed to Euclidean space that suggests that fourth- dimension is abstraction. Therefore, 4-D are often generated

*Corresponding author. Tel: +60-166766807
*Email address: magedupm@hotmail.com

algebraically, by utilizing the rules of vectors and coordinate geometry to a space in 4-D (Anne, 2013; Marghany, 2014).

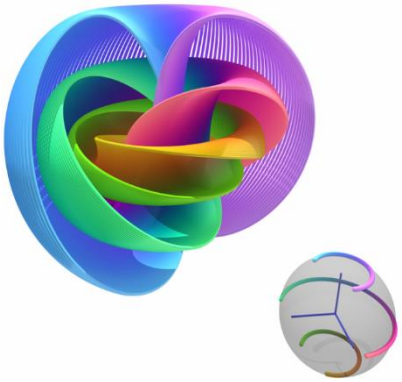

Figure 1: Four-dimensional

Nonetheless, there are excellent advances in remote sensing technology which might offer 3-D maps through LIDAR, TanDAM TerraSAR –X etc., the human eyes are restricted to look at 2-D or 3-D objects and ineffective to be viewed in n-dimension. In free space universe, there are parallel coordinates which might view the universe in n-dimensional. One among the accurate remote sensing technique for 3-D visualization is interferometry synthetic aperture radar techniques. Yet, the performance of interferometric section estimation suffers seriously from poor image coregistration. Interferogram filtering algorithms like adaptational contoured window, pivoting mean filtering, pivoting median filtering, and accommodative phase noise filtering are the most methods for the standard InSAR interferometric phase estimation (Pepe 2012). Recently, Marghany (2011) enforced holograph interferometry for bound amendment. Marghany (2014) introduced a brand new technique to reconstruct 4-D from holograph interferometry for optical remote sensing and ENVISAT ASAR knowledge. Though, these studies does not explained clearly the mathematical formulas accustomed reconstruct 4-D. Truly, 4-D is necessary to formulate mathematical protocols to be implemented in many applications (Marghany, 2015).

The foremost enquiry is the way to reconstruct 4-D from 3-D? This study postulates that 4-D is implicit from 3-D phase unwrapping of optical holograph interferometry. As a matter of reality, optical interferometry could be a powerful approach to live shifts of the soundness of electromagnetic wavelength spectra. One vital limitation of common interferometric strategies is that they need reflective reflectors. This limitation is detached by utilizing optics, permitting terribly tiny motions of impulsive, diffusely reflective, objects to be detected. The most novelty of this study is to derive a replacement formula for 4-D holograph interferometry phase unwrapping Hybrid Genetic algorithmic program (HGA) within which are often enforced to determine the tidal wave damages. This could be delineated by deep visualisation on the sting of objects (Marghany, 2015). The mainly objective is to reconstruct fourth-dimensional of 2004 tsunami impacts on Kalutara coastline from high resolution QuickBird satellite data by optimization of 4-D holograph interferometry.

2. Search Area and Data Acquisition

Kalutara lineation is found in Sri Lanka between latitude of 6°34’21.03” N to 6°34’ 57.28” N and longitude of 79°57’ 13.63” E to 79°58’ 04.87” E (Figure 2). Moreover, Sri Lanka is dominated by two monsoon periods. Indeed, southwest monsoon brings that rain principally from might to July to the western, southern and central regions of the Sri Lanka Island, whereas the northeast monsoon rains occur within the northern and eastern regions in December and January that square measure influenced the coast of Sri Lanka often.

Figure 2: Kalutara coastline

In this study, the high-resolution QuickBird satellite data were acquired from Digital Global archives data. The images of QuickBird were acquired before, and after tsunami disaster of Kalutara coastline. The multispectral QuickBird satellite data within less than 1 m pixel resolution is chosen. For ocean wave spectra extraction the composite color bands of 450-520 nm (blue), 520-600 nm (green), and 630-690 nm (red) is used. The multispectral QuickBird satellite was acquired on Sunday December 26, 2004, at 10:20 am local time, slightly less than four hours after the 6:28 a.m. (local Sri Lanka time) earthquake and shortly after the moment of tsunami impact.

3. 4-D Hologram Interferometry

The procedures of 4-D hologram interferometry are comprehended in Figure 3. Resulting Marghany (2015), presume that I_1 and I_2 are the two different acquisition times of satellite data as an example, QuickBird satellite data.

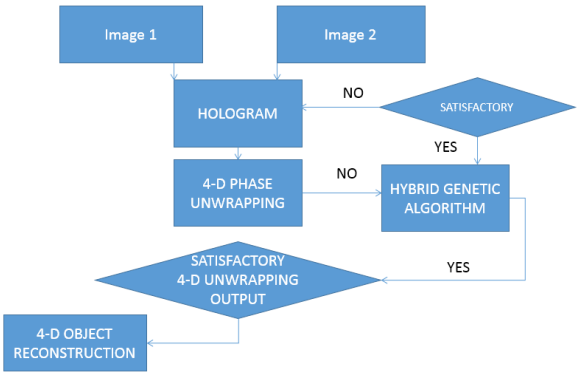

Figure 3: Hologram interferometry procedures

Consequently, $I_1 \in E_1$ and $I_2 \in E_2$ where $E_1 \notin E_2$ or $E_1 \neq E_2$ as E is electromagnetic spectra that presents in two QuickBird satellite information. Each electromagnetic spectra waves interfere at the surface of purpose in space or time. Hence, their amplitudes can add as vector. If one amongst these could be a plane wave inform within the z direction and therefore the alternative could be a spherical wave, then it can delineated by:

$$I(x,y) = |E(x,y)\, e^{(i\phi O(x,y))} + r(x,y)\, e^{(i\phi R(x,y))}|$$
$$= (E_2(x,y)\, e^{(i\phi R(x,y))})(r(x,y)\, e^{(i\phi R(x,y))})^* + (E_1(x,y)\, e^{(i\phi O(x,y))})(E(x,y)\, e^{(i\phi O(x,y))})^*$$
$$+ (E_1(x,y)\, e^{(i\phi O(x,y))})(E_2(x,y)\, e^{(i\phi R(x,y))})^* + (E_2(x,y)\, e^{(i\phi R(x,y))})(E_1(x,y)\, e^{(i\phi O(x,y))})^* \quad (1)$$

where ***E*** is the is the complex amplitude of the object wave with real amplitude E_1 and phase ϕO , $\mathbf{E_2}$ is the complex amplitude of the reference wave with real amplitude E_2 and phase ϕR and * denotes the conjugate complex. The phase changes due to deformation can be obtained by using 2-DFFT into the above equation [21]

$$FFT\{I\} = A(f_x + f_y) + B(f - f_x, f - f_y)B^*(f - f_x, f - f_y) \quad (2)$$

where FFT denote the Fourier spectra and *f* is that the spatial frequency within the *x* and *y* directions, are the carry frequencies within the *x* and *y* directions, severally. Comprehending de la Torre et al.,(2010), 4-D holographic interferometry (HI) is given by

$$FFT\{I_N\} = \sum_{N=1}^{4}[A_N(f_x + f_y + f_z) + B_N(f - f_{Nx}, f - f_{Ny}, f - f_{Nz}) + B_N{}^*(f - f_{Nx}, f - f_{Ny}, f - f_{Nz})] \quad (3)$$

where *N* denotes 4-D, A_N is the incoherent in 4-D holographic interferometry. B_N and $B_N{}^*$ are lobes for every illumination wavelength in QuickBird satellite data. The relative optical part distinction are often associated to a physical displacement through the sensitivity vector found within the holograph interferometry in two satellite data which might be expressed in 4-D as,

$$\begin{pmatrix}\Delta\Phi_1\\ \Delta\Phi_2\\ \Delta\Phi_3\\ \Delta\Phi_4\end{pmatrix} = \frac{2\pi}{\lambda}\begin{pmatrix}\vec{d}_{1i} & \vec{d}_{1j} & \vec{d}_{1k} & \vec{d}_{1p}\\ \vec{d}_{2i} & \vec{d}_{2j} & \vec{d}_{2k} & \vec{d}_{2p}\\ \vec{d}_{3i} & \vec{d}_{3j} & \vec{d}_{3k} & \vec{d}_{3p}\\ \vec{d}_{4i} & \vec{d}_{4j} & \vec{d}_{4k} & \vec{d}_{4p}\end{pmatrix}\begin{pmatrix}U\\ V\\ W\\ O\end{pmatrix} \quad (4)$$

Subsequent Marghany (2015), *d* is the dislocation in along orthogonal components of *U*,*V*,*W*,*O*, in *i*,*j*,*k*, and *p*, correspondingly. On the word of Marghany (2015), phase unwrapping can be extended into fourth-dimensional by the given equation,

$$\sum_{i,j,k,p} W^x_{i,j,k,p}\left|\Delta\phi^x_{i,j,k,p} - \Delta\psi^x_{i,j,k,p}\right|^L + \sum_{i,j,k,p} W^y_{i,j,k,p}\left|\Delta\phi^y_{i,j,k,p} - \Delta\psi^y_{i,j,k,p}\right|^L + \sum_{i,j,k,p} W^z_{i,j,k,p}\left|\Delta\phi^z_{i,j,k,p} - \Delta\psi^z_{i,j,k,p}\right|^L + \sum_{i,j,k,p} W^z_{i,j,k,p}\left|\Delta\phi^w_{i,j,k,p} - \Delta\psi^w_{i,j,k,p}\right|^L \quad (5)$$

where $\Delta\phi$ and $\Delta\psi$ are the unwrapped and wrapped phase differences in *x*,*y*,*z*,*w* correspondingly, and W signifies user-defined weights. The summations are carried out in both *x* ,*y*, *z*, and *w* directions over all *i*,*j*,*k*, and *p*, respectively.

The hybrid genetic algorithm (HGA) counts on approximating the constraints of an n^{th} order-polynomial to estimate the unwrapped surface clarification from the wrapped phase data (Karout, 2007; Marghany, 2015).

Any optimization drawback employing a genetic algorithmic program (GA) needs the matter to be coded into GA syntax type, that is the chromosome type. During this downside, the chromosome consists of variety of genes wherever each gene correspond to a constant within the nth-order surface fitting polynomial this may be extended into 4-D as follows (Marghany, 2015):

$$f := n \to \sum_{p=0}^{n} \sum_{k=0}^{n} \sum_{j=0}^{n} \sum_{i=0}^{n} a_{i,j,k,p} \Delta\phi_{i,j,k,p}^{x} \Delta\phi_{i,j,k,p}^{y} \Delta\phi_{i,j,k,p}^{z} \Delta\phi_{i,j,k,p}^{w} \quad (6)$$

where $a[0....n]$ are the parameter coefficients which are retrieved by the genetic algorithm to approximated the unwrapped phase. Further, *i,j, k* and *p* are indices of the pixel location in the unwrapped phase in 4-D, respectively, *n* is the number of coefficients.

The correct 4-D phase unwrapping are often obtained by phase matching algorithmic rule that is usually recommended by Schwarz (2004). In keeping with Schwarz (2004), phase matching algorithmic program is matched the phase of wrapped phase with unwrapped phase by the given equation

$$\psi_{i,j,k,p} = \Delta\phi_{i,j,k,p} + 2\pi\rho\left[\frac{1}{2\pi}\left(\hat{\Delta\phi}_{i,j,k,p} - \Delta\phi_{i,j,k,p}\right)\right] \quad (7)$$

As stated by Schwarz (2004);Pepe (2012); Marghany (2015), the phase matched unwrapped phase in the caratsin coordinate *i,j,*and *k* in the quality phase map is $\psi_{i,j,k,p}$. However, $\Delta\phi_{i,j,k,p}$ denotes the wrapped phase. Consequently, $\rho[.]$ is a rounding function which is defined by $\rho[t] = \lfloor t + 1/2 \rfloor$ for $t \geq 0$ and $\rho[t] = \lfloor t - 1/2 \rfloor$ for $t < 0$ and are *i,j, k* and *p* the pixel positions in *x* and *y,z,w* directions, respectively. Finally, $\hat{\Delta\phi}_{i,j,k,p}$ is the estimated unwrapped phase.

4. Result and Discussion

The earthquake and therefore the tidal wave, that smitten the lineation of the Indian Ocean and Sumatra, Indonesia on 26 December 2004, have caused huge changes within the shorelines of the many countries particularly in Banda Aceh, Indonesia and Kalatura, Sri Lanka. Scientists work the harm in Aceh found proof that the wave reached a height of 80 feet (24 m) once returning toward land on massive stretches of the lineation, rising to 100 feet (30 m) in some areas once traveling landlocked. This deadliest disaster has caused large destruction to the surroundings and also the world ecosystems despite killing millions of individuals everywhere the globe. Figure 4 shows the two QuickBird satellite data were no inheritable over Kalutara lineation pre tsunami and post tsunami event, correspondingly.

Apparently, vast damages are caused by 2004 box-day tidal wave (Figure 4b). This is often contributed attributable to indisputable fact that QuickBird satellite has multispectral sensors with 0.61 m-0.72 m and 2.44m –2.88 m resolution severally, counting on the off-nadir viewing angle (0-25 degrees). The device thus has coverage of 16.5 km within the across-track direction. Additionally, the along-track and across-track capabilities offer sensible stereo geometry and a high revisit frequency of 1-3.5 days. These characteristics of the pictures modify straightforward management and observation of earth particularly for disaster observation and mapping like wave disaster.

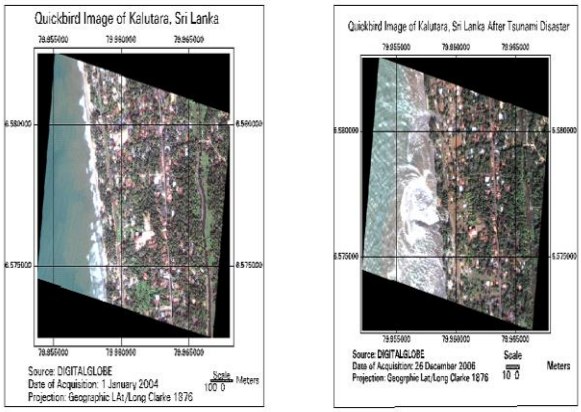

(a) (b)

Figure 4: QuickBird satellite data pre and post tsunami Events along Kalutara (a) January 1, 2004, and (b) December 26, 2004

The contrast between 2-D phase unwrapping; 3-D phase unwrapping; and 4-D phase unwrapping is exposed in Figure 5. The holograph interferometry fringes pattern are additional vibrant by exploitation 4-D phase unwrapping as compared to different phase unwrapping dimensions i.e. 2-D and 3-D. Figure 6 shows the 4-D visual image derived from holograph interferometry. Obviously, the 4-D visual image distinguishes between infrastructures and buildings. With this regard, coding 2-D of QuickBird data into 4-D will visualize several data concerning urban options i.e. building, infrastructures, and roads in spite of the great damages caused by tsunami.

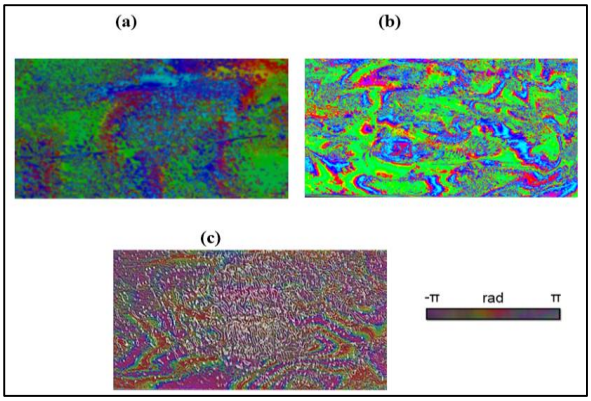

Figure 5: Phase unwrapping (a)2-D;(b)3-D; and (c) 4-D

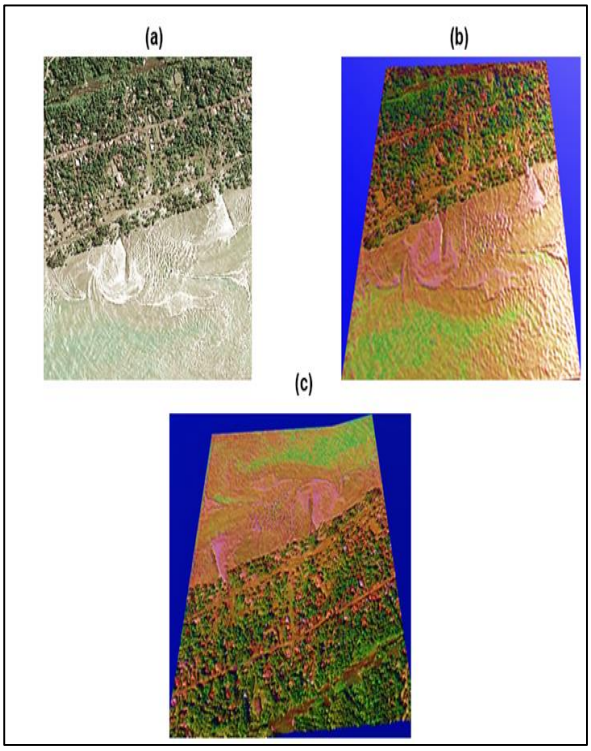

Figure 6:4-D visualization produced by 4-D hologram interferometry (a) original data; (b) 90°; and (c) 180 °

Particularly, the entire cycle of holograph interferometry fringe patterns are bound with 4-D phase unwrapping algorithmic program. With this regard, 4-D holographic interferometry fringes created by exploitation Hybrid Genetic algorithmic rule supported Pareto optimal Solutions. It is attention-grabbing to seek out that the planned algorithmic rule has made clear options detection of infrastructures.

In fact, the planned algorithmic program has reduced the error in interferogram cycle due the low coherence in water and vegetation zones and on the lineation owing to tidal wave impact. This might be improvement of such previous work of Hussein et al. (2005); Karout(2007); and Marghany (2015).

Indeed, the holograph interferometry is taken into account as a deterministic algorithmic program that is delineated here to optimize a triangulation domestically between two completely different points. This corresponds to the feature of deterministic methods of finding solely sub-optimal solutions typically. This confirms that optical interferometry may be a sturdy suggests that for evaluating displacements of the order of a wavelength of electromagnetic spectra. Therefore, involving a holograph can assist in recovering the matter of reflective reflection beside allowing little changes of random, diffusely replication, objects to be known (Saxby, 1987).

Along with Karout (2007) and Saravana et al., (2003) a genetic algorithm is used to approximate the coefficient of an n^{th}-order polynomial which is considered as best estimates for the unwrapped phase map. With this regard, it minimizes the variance between the unwrapped phase gradient and the wrapped phase gradient. Furthermore, 4-D results obtained with the hybrid genetic algorithm exceed the performance of the 4-D phase unwrapping of hologram interferometry. The visualization of the infrastructures is sharp by 4-D phase unwrapping based Hybrid Genetic Algorithm.

These results delivers a superb promising for 4-D reconstruction exploitation 4-D phase unwrapping of holograph interferometry. This study is rising the work done by Marghany (2015). Moreover, the adding fourth coordinate p in mathematical formula of 3-D holograph interferometry (HI) formed a superb 4-D object visual image. Hybrid genetic rule (HGA) assists to deliver 4-D image and not solely discriminating the individual relaxed deformation nevertheless conjointly finding out hindering objects in 4-D. Commonly, hybrid genetic algorithmic rule (HGA) matches the phase of the wrapped phase with guessed unwrapped phase to verify the most effective illustration of the unwrapped phase.

5. Conclusions

The 4-D phase unwrapping approaches delineated are applicable to reconstruct 4-D visual image of tsunami effects exploitation QuickBird satellite data. The involving of hybrid genetic algorithmic rule to optimize modification formula of holograph interferometry can tolerate the QuickBird satellite data to be coded into 4-D. The results exposes that the forms of 2-D objects in QuickBird data is visualized in 4-D. The fine limits of

roads, urban, buildings and infrastructures are well projected in 4-D. Lastly, the modification and improvement of holograph interferometry formula hold tremendous promises for 4-D object visual image in such optical satellite data of QuickBird.

References

Alday, L., Gaiotto, D. and Tachikawa, Y. (2010). 'Liouville correlation functions from four-dimensional gauge theories'. Letters in Mathematical Physics, 91 (2), pp. 167–197.

Anne, D.W. (2013). 'Moral Authority, Men of Science, and the Victorian Novel'. Cambridge University Press.

Haupt, R.L. and Haupt, S.E. (2004). 'Practical genetic algorithms'. John-Wiley & Sons.

Hussein, S.A., Gdeist, M., Burton, D. and Lalor, M. (2005). 'Fast three-dimensional phase unwrapping algorithm based on sorting by reliability following a non-continuous path'. Proc. SPIE, 5856, 40.

Karout, S. (2007). 'Two-dimensional Phase Unwrapping, Ph.D. Theses, Liverpool John Moores University, 2007.

Kohli, D., Richard, S., Norman, K. and Stein, A. (2012). 'An ontology of slums for image-based classification. Computers'. Environment and Urban Systems, 36 (2), pp. 154–163.

Marghany, M. (2003). 'Polarised AIRSAR along track interferometry for shoreline change modeling'. In *Geoscience and Remote Sensing Symposium, 2003. IGARSS'03. Proceedings. 2003 IEEE International*, Vol. 2, pp. 945-947.

Marghany, M. (2011).'Modelling shoreline rate of changes using holographic interferometry'. *Int. J. of Phys. Sci*, *6*, pp. 7694-7698.

Marghany, M. (2012). Simulation of 3-D coastal Spit Geomorphology Using Differential Synthetic Aperture Interferometry (DInSAR). In I. Padron, (ed.) Recent Interferometry Applications in Topography and Astronomy. Croatia: InTech – Open Access Publisher, (2012) 83-94.

Marghany, M. (2013). 'DInSAR technique for three-dimensional coastal spit simulation from radarsat-1 fine mode data'. Acta Geophysica .61, 2, 478-493.

Marghany, M. (2014).'Hologram interferometric SAR and optical data for fourth-dimensional urban slum reconstruction'. CD of 35th Asian Conference on Remote Sensing (ACRS 2014), Nay Pyi Taw, Myanmar 27- 31, October 2014,http://www. a-a-rs.org/acrs/administrator/components/com.../OS-303%20.pdf.[Access on August 2 2016].

Marghany, M. (2014a). 'Simulation of three-Dimensional of coastal erosion using differential interferometric synthetic aperture radar'. Global NEST Journal, 16: 1: pp 80-86.

Marghany, M. (2014b). 'Hybrid genetic algorithm of interferometric synthetic aperture radar for three-dimensional coastal deformation'. Frontiers in artificial intelligence and applications: new trends in software methodologies, tools and technique, 265, 116-31.

Marghany, M. (2015). 'Fourth dimensional optical hologram interferometry of RapidEye for Japan's tsunami effects'. CD of 36th Asian Conference on Remote Sensing (ACRS 2015), Manila, Philippines, 24-28 October 2015.

Pepe, A. (2012). 'Advanced multitemporal Phase Unwrapping Techniques for DInSAR Analyses'. In Padron I. (ed.) 'Recent interferometry applications in topography and astronomy'. InTech - Open Access Publisher, University Campus STeP Ri, Croatia. (2012), 57-82.

Ray, I. (1992). 'Introducing Einstein's Relativity'. Clarendon Press, chp. 22.8 Geometry of 3-spaces of constant curvature, p.319ff.

Saravana, S., Ponnanbalam, S.G. and Rajendran, C.A. (2003). 'Multi-objective genetic algorithm for scheduling a flexible manufacturing system'. International Journal of Advanced Manufacturing Technology, 22, 229-236.

Saucedo, A.T., De la Torre-Ibarra, M. H., Santoyo, F. M. and Moreno, I. (2010). 'Digital holographic interferometer using simultaneously three lasers and a single monochrome sensor for 3D displacement measurements'. Optics express, 18(19), pp. 19867-19875.

Saxby, G. (1987).'Practical Holography'. Prentice Hall,NJ.

Schwarz, O. (2004). 'Hybrid phase unwrapping in laser speckle interferometry with overlapping windows'. Shaker Verlag.

Smith, J. (2010). 'Optimizing remote sensing for disaster monitoring'. Retrieved May 13, 2005, from http://www.remotesening.net/index.htm.

Takeda, M., Ina, H. and Kobayashi, S. (1982). 'Fourier-transform method of fringe-pattern analysis for computer-based topography and interferometry'. *JosA*, *72*(1), pp.156-160.